SCIENCE CHINA
Information Sciences

• RESEARCH PAPER •

February 2018, Vol. 61 022306:1–022306:15
doi: 10.1007/s11432-016-9143-6

Energy-efficient cell-association bias adjustment algorithm for ultra-dense networks

Wenxiang ZHU[1], Pingping XU[1*], ThiOanh BUI[1], Guilu WU[1] & Yan YANG [2]

[1]*National Mobile Communications Research Laboratory, Southeast University, Nanjing* 210096*, China;*
[2]*Department of Electronic and Electrical Engineering, Bengbu University, Bengbu* 233030*, China*

Received 31 October 2016/Revised 25 February 2017/Accepted 24 May 2017/Published online 25 August 2017

Abstract In recent years, energy efficiency has become an important topic, especially in the field of ultra-dense networks (UDNs). In this area, cell-association bias adjustment and small cell on/off are proposed to enhance the performance of energy efficiency in UDNs. This is done by changing the cell association relationship and turning off the extra small cells that have no users. However, the variety of cell association relationships and the switching on/off of the small cells may deteriorate some users' data rates, leading to nonconformance to the users' data rate requirement. Considering the discreteness and non-convexity of the energy efficiency optimization problem and the coupled relationship between cell association and scheduling during the optimization process, it is difficult to achieve an optimal cell-association bias. In this study, we optimize the network energy efficiency by adjusting the cell-association bias of small cells while satisfying the users' data rate requirement. We propose an energy-efficient centralized Gibbs sampling based cell-association bias adjustment (CGSCA) algorithm. In CGSCA, global information such as channel state information, cell association information, and network load information need to be collected. Then, considering the overhead of the messages that are exchanged and the implementation complexity of CGSCA to obtain the global information in UDNs, we propose an energy-efficient distributed Gibbs sampling based cell-association bias adjustment (DGSCA) algorithm with a lower message-exchange overhead and implementation complexity. Using DGSCA, we derive the updated formulas for calculating the number of users in a cell and the users' SINR. We analyze the implementation complexities (e.g., computation complexity and communication complexity) of the proposed two algorithms and other existing algorithms. We perform simulations, and the results show that CGSCA and DGSCA have faster convergence speed, as well as a higher performance gain of the energy efficiency and throughput compared to other existing algorithms. In addition, we analyze the importance of the users' data rate constraint in optimizing the energy efficiency, and we compare the energy efficiency performance of different algorithms with different number of small cells. Then, we present the number of sleeping small cells as the number of small cells increases.

Keywords ultra-dense networks, cell-association bias, energy efficiency, Gibbs sampling, users' data rate constraint

Citation Zhu W X, Xu P P, Bui T O, et al. Energy-efficient cell-association bias adjustment algorithm for ultra-dense networks. Sci China Inf Sci, 2018, 61(2): 022306, doi: 10.1007/s11432-016-9143-6

1 Introduction

Driven by the exponential growth of wireless traffic requirements, network operators have to address 1000x network capacity demands in fifth-generation (5G) networks [1]. A promising solution for 5G networks is ultra-dense networks (UDNs), which can improve the network capacity and coverage performances via infrastructure densification [2]. In UDNs, ultra dense low-power and low-cost small cells are co-channel

* Corresponding author (email: xpp@seu.edu.cn)

deployed in the coverage area of macrocells, which brings not only opportunities but also challenges. The opportunities result from the higher service quality offered to users arising from the reuse of the frequency spectrum, while the challenges refer to the serious inter-cell interference (ICI) and the load imbalance among cells [3, 4]. Besides, with the large-scale deployment of small cells in UDNs, the energy consumption of networks increases rapidly [5].

According to the statistics reported by manufacturers and network operators, in each year, 60 billion kWh of electric energy are consumed by cellular networks, 65% of which is related to base station operations [6]. In order to alleviate the negative effort of the network on energy savings, the international collaborative project, the energy aware radio and network technologies (EARTH), was initiated, and there have been significant efforts to develop green communication technologies to improve the energy efficiency, which is defined as the ratio of the throughput to the energy consumption of the network [7].

There have been many valuable contributions on UDNs and energy efficiency. In [8], the authors propose a distributed network architecture for 5G ultra-dense cellular network, and they investigated the impact of backhaul network capacity and backhaul energy efficiency on the network densification. In [9], the users' mobility performance, e.g., the user pause probability, user arrival, and departure probability, is investigated in the 5G small cell network based on individual mobility models, and they derive the coverage probabilities of the small cells and the macrocell. In early studies, the authors focused on the transmission power optimization to maximize the energy efficiency. In [10], a unique optimallink adaptive transmission scheme is derived to maximize the energy efficiency. However, the EARTH technical report implies that the transmission power is responsible for only a small portion of the energy consumption of a small cell [11]. In other words, by adjusting the transmission power of the small cells, we can realize only a small reduction in energy consumption. The small cell on/off technique is a more efficient method to realize energy savings and improve the energy efficiency. This technique can transfer users between base stations and turn off the small cells in an energy-efficient way. For this reason, the small cell on/off scheme and cell association algorithm are usually jointly considered. Some works studied the energy efficiency optimization problem by changing the cell association and turning off the small cells that have no users. Applying the stochastic geometry theory, the authors in Ref. [12] derived the closed-form expressions of the optimal base station density to minimize the area power consumption and analyzed the optimal type of base stations to be deployed or turned off. From the perspective of the optimization algorithm, in [13], the cell association and resource allocation are jointly optimized to maximize the energy efficiency under the fixed small cell on/off mode, and then the small cell operation pattern is iteratively optimized.

The reference signal received power (RSRP)-based cell association scheme [14] and bias-based cell association scheme [15] are two basic cell association schemes that are investigated for cellular networks. Owing to the strong downlink interference resulting from high power macrocells, under the conventional cell association method based on the maximum RSRP, the coverage of the small cells has decreased, which leads to a gross underutilization of small cells and limits the network spectrum/energy efficiency improvement [16]. The energy efficiency can be improved by optimizing the conventional binary decision on the cell association relationship, but the computational complexity is high and the method is sensitive to changes in the network topology. A simple and efficient bias-based cell association method is proposed in [17]. In the bias-based cell association scheme, an artificial bias is added to each cell, and each user is associated with the cell, which provides the maximum biased reference signal receiving power (BRSRP) [18]. By setting a positive cell-association bias value, a small cell can offload users from the heavy load macrocell and surrounding small cells, which appears as if the coverage range of the small cell is expanded and more resources are made available to offloaded users. If the benefits of resources resulting from the user transfer can mitigate for the SINR degradation, then the network throughput can be improved. In contrast, if the cell-association bias of a small cell is negative, the users of the small cell will be transferred to the macrocell or to its surrounding small cells, and the source small cell can be switched to sleep mode to reduce the energy consumption of the network if all of its traffic is offloaded. In summary, from an energy efficiency perspective, the cell-association bias optimization can both improve the system throughput through the optimized resource reallocation and can reduce the energy consumption of the network through small cell sleeping, which can ultimately promote the energy

efficiency of the network.

The bias-based cell association schemes can be summarized as the following two classical patterns: the tier-specific cell-association bias scheme and the cell-specific cell-association bias scheme. In the tier-specific cell-association bias scheme, the small cells in each tier have an identical cell-association bias. However, this scheme is only efficient when the traffic or user distribution between different small cells is almost identical. When the traffic or user distribution between different small cells differs significantly, the efficiency of the tier-specific cell-association bias-based scheme becomes low [19]. In the cell-specific cell-association bias scheme, each small cell, even those within the same tier, has a different cell-association bias, which addresses the scenario where there are differences among small cells [20].

In this paper, we focus on the scenario of the cell-specific cell-association bias. In [21], the authors jointly optimized the transmission power and the cell-specific cell-association bias to alter the user association, and they turned off the extra small cells to maximize the energy efficiency of the small cells. However, the cell-association bias was assumed to be a continuous optimization variable, and the users' data rate constraint was not taken into consideration. In practice, in the 3GPP standards, the recommended cell-association bias setting is discrete and each user has its own data requirement [22]. Considering that biased users may experience unfavorable channels and suffer from strong interference from the original base station, the ability to improve the energy efficiency is relative to the selected cell-association bias values. Therefore, it remains a problem of how to maximize the energy efficiency by optimizing the discrete cell-association bias, while meeting the users' data rate requirement.

Because of the increasing density of small cells, existing cell association algorithms cannot be applied to the UDNs owing to the large information-exchange overhead, high computation complexity, and slow convergence speed. As a reinforcement-learning approach, Gibbs sampling can be used to solve the discrete optimization problems with low computation complexity and fast convergence speed. For instance, it can be used to maximize the sum of the user rates in cognitive radio networks [23], and can maximize the system throughput and proportional fairness in wireless sensor networks [24]. In [25], the authors studied the Gibbs sampling and the variant Metropolis-Hastings (MH) algorithm, and they proposed an enhanced MH algorithm with a priori known target state distribution to improve the convergence speed. To the best of our knowledge, Gibbs sampling has not been used to optimize the cell-association bias for energy efficiency, while satisfying the users' data rate requirement in UDNs.

As discussed above, in this paper, we first formulate an energy efficiency optimization problem considering the users' data rate constraint and the discrete cell-association bias criteria. Then, we propose two energy-efficient Gibbs sampling based cell-association bias adjustment algorithms to solve the optimization problem. The first one is the centralized Gibbs sampling based cell-association bias adjustment (CGSCA) algorithm, in which the central macrocell makes the decision using the global information, such as channel state information, network load information, and cell-association information. After that, considering the overhead of the exchanged messages and the implementation complexity of CGSCA to obtain these sets of information, we propose a distributed Gibbs sampling based cell-association bias adjustment (DGSCA) algorithm by adopting the local information, and we derive the information about the updated number of users and SINR are derived. Finally, we analyze the communication complexity and communication overhead, and we perform numerous simulations.

The remainder of this paper is organized as follows. In Section 2, we introduce the system model of a two-tier UDN. Then, in Section 3, we formulate the energy efficiency maximization problem and analyze the NP-hardness of the problem. In Section 4, we propose the energy-efficient Gibbs sampling based cell-association bias adjustment algorithm, which includes the original Gibbs sampling algorithm, CGSCA and DGSCA algorithms. In Section 5, we analyze the computational complexity and the communication complexity of the proposed algorithms, and in Section 6, we present the system level simulations, including the simulation parameters and results. Finally, we conclude the paper in Section 7.

2 System model

Consider a downlink co-channel OFDM macrocell-picocell UDN scenario where there exists N_M macrocells,

N_P picocells, and N_U users. The set of cells is $\mathcal{C} = \{\mathcal{M} \cup \mathcal{O}\}$, where $\mathcal{M} = \{M_1, M_2, \ldots, M_{N_M}\}$ is the set of macrocells and $\mathcal{O} = \{O_1, O_2, \ldots, O_{N_P}\}$ is the set of picocells. The set of users is $\mathcal{U} = \{U_1, U_2, \ldots, U_{N_U}\}$. We applied the cell-specific cell-association bias-based cell association criteria, and the feasible cell-association bias value is discrete. The set of cell-association bias is $\mathcal{B} = \{B_{\min}, B + \Delta, \ldots, B_{\max}\}$, where Δ is the adjustment interval of the cell-association bias, and $B_{\max}$ and $B_{\min}$ are the maximum and the minimum cell-association bias value, respectively. We adopted the open-access mode as the access criterion so that the users can select any cell as their serving cell. We denote the transmission power of cell i as P_i, and the RSRP $P_{i,k}^{\text{rec}}$ of user k from cell i can be calculated as

$$P_{i,k}^{\text{rec}} = P_i G_{i,k}, \quad i \in \mathcal{C}, k \in \mathcal{U}, \tag{1}$$

where $G_{i,k}$, which consists of the antenna gain, shadow fading, and path loss, is the average channel gain between cell i and user k. To avoid frequent handovers, in a practical system, the users' serving cell cannot be continuously changed [26]. Considering that the cell-association bias adjustment has a coupled relationship with the serving cell decision of the users, the cell-association bias adjustment should be carried out over a large time scale that is much slower than the time scale of small-scale fading. Therefore, as in other related studies [24, 27, 28], small-scale fading was not considered in the calculation of the average channel gain.

The cell-association bias is only employed in each small cell. In other words, the cell-association bias for a macrocell i $(i \in \mathcal{M})$ is $B_i = 0$ dB, and that for a picocell i $(i \in \mathcal{O})$ is $B_i \in \mathcal{B}$. The users' serving cell association criteria based on BRSRP can be expressed as

$$\zeta_k(\mathcal{B}) = \arg\max_{i \in \mathcal{C}} \left(P_{i,k}^{\text{rec}} + B_i\right), \tag{2}$$

where $\zeta_k(\mathcal{B})$ is the serving cell of user k under the bias set $\mathcal{B}$. The SINR of user k associated with cell ζ_k is

$$\gamma_{k,\zeta_k}(\mathcal{B}) = \frac{P_{\zeta_k} G_{\zeta_k,k}}{\sum_{i \in \mathcal{C}/\zeta_k} P_i G_{i,k} + N_0}, \tag{3}$$

where P_{ζ_k} and P_i are the transmission power of the serving cell and interference cell of user k, respectively. N_0 is the noise power.

The bandwidth of each cell is a constant denoted as W. There are two factors that affect the bandwidth allocation of user k. The first is the number of users Z_{ζ_k} in user k's serving cell ζ_k, and the other is the SINR $\gamma_{k,\zeta_k}(\beta)$ of user k. Therefore, the allocated bandwidth of user k is

$$W_k\left(Z_{\zeta_k}(\mathcal{B}), \gamma_{k,\zeta_k}(\mathcal{B})\right) = f_W\left(Z_{\zeta_k}(\mathcal{B}), \gamma_{k,\zeta_k}(\mathcal{B})\right), \tag{4}$$

where W_k is the bandwidth allocation of user k. From the perspective of fairness and throughput, Ref. [27] proved that the optimal bandwidth allocation for the large time-scale condition is to have an equal bandwidth allocation among all users. Therefore, we adopt the equal-bandwidth allocation scheme for each user, and the bandwidth allocation of user k can be expressed as $W_k\left(Z_{\zeta_k}(\mathcal{B})\right) = W/Z_{\zeta_k}(\mathcal{B})$. According to the Shannon expression, the achievable data rate of user k can be represented as

$$R_k\left(Z_{\zeta_k}(\mathcal{B}), \gamma_{k,\zeta_k}(\mathcal{B})\right) = W_k\left(Z_{\zeta_k}(\mathcal{B})\right) \log_2\left(1 + \gamma_{k,\zeta_k}(\mathcal{B})\right). \tag{5}$$

We denote R_i as the total achievable data rate of users for cell i, and the network throughput can be calculated by

$$\text{Thput}\left(\mathcal{Z}(\mathcal{B}), \gamma(\mathcal{B})\right) = \sum_{i \in \mathcal{C}} R_i = \sum_{i \in \mathcal{C}} \sum_{k \in i} R_k\left(Z_{\zeta_k}(\mathcal{B}), \gamma_{k,\zeta_k}(\mathcal{B})\right), \tag{6}$$

where $\mathcal{Z}(\mathcal{B})$ and $\gamma(\mathcal{B})$ are the sets of the number of users and the SINR under the cell-association bias set $\mathcal{B}$ of the whole network, respectively.

Using the liner approximation energy consumption model given by [11], the energy consumption of macrocell v and picocell c are

$$P_{\text{M\_com}}^{v} = P_M^0 + \Delta_M P_M^v, \tag{7}$$

$$P_{\mathrm{P\_com}}^{c}\left(Z_c\left(B_c\right)\right)=\begin{cases}P_P^0+\Delta_P P_P^c, & \text{if } Z_c\left(B_c\right)>0,\\ P_P^S, & \text{if } Z_c\left(B_c\right)=0,\end{cases} \tag{8}$$

where P_M^0 and P_P^0 are the energy consumption of the macrocell and picocell in the idle state, respectively. P_M and P_P are the transmission power of the macrocell and picocell, respectively. Δ_M and Δ_P are the reciprocal of the power amplifier efficiency of the macrocell and picocell, respectively, and P_P^S is the energy consumption of the picocell in the sleep state. The energy consumption of the whole network can be calculated by

$$P_{\mathrm{total}}\left(\mathcal{Z}\left(\mathcal{B}\right)\right)=\sum_{v\in\mathcal{M}}\left(P_M^0+\Delta_M P_M^v\right)+\sum_{c\in\mathcal{O}}\left[\left(P_P^0+\Delta_P P_P^c\right)L_c\left(B_c\right)+P_P^S\left(1-L_c\left(B_c\right)\right)\right], \tag{9}$$

where L_c is a traffic indicator. If the number of users in the cell c is zero, i.e., $Z_c\left(B_c\right)=0$, the traffic indicator $L_c\left(B_c\right)=0$; otherwise, $L_c\left(B_c\right)=1$. The network energy efficiency η_{EE} can be expressed as

$$\begin{aligned}\eta_{EE}(\mathcal{Z}(\mathcal{B}),\gamma(\mathcal{B}))&=\frac{\mathrm{Thput}(\mathcal{Z}(\mathcal{B}),\gamma(\mathcal{B}))}{P_{\mathrm{total}}(\mathcal{Z}(\mathcal{B}))}\\&=\frac{\sum_{i\in\mathcal{C}}\sum_{k\in i}R_k(Z_{\zeta_k}(B_{\zeta_k}),\gamma_{k,\zeta_k}(B_{\zeta_k}))}{\sum_{v\in\mathcal{M}}(P_M^0+\Delta_M P_M^v)+\sum_{c\in\mathcal{O}}\left[(P_P^0+\Delta_P P_P^c)L_c(B_c)+P_P^S(1-L_c(B_c))\right]}.\end{aligned} \tag{10}$$

3 Problem formulation

Aiming at finding the global best cell-association bias set $\mathcal{B}^*$ to maximize the network energy efficiency while satisfying the constraint of users' data rate requirements and discrete cell-association bias criteria, we formulated the optimization problem as

$$\arg\max_{\mathcal{B}}\ \eta_{EE}\left(\mathcal{Z}\left(\mathcal{B}\right),\gamma\left(\mathcal{B}\right)\right), \tag{11a}$$

$$\text{s.t. } B_i=0, i\in\mathcal{M}, \tag{11b}$$

$$B_i\in\mathcal{B}, i\in\mathcal{O}, \tag{11c}$$

$$\zeta\left(\mathcal{B}\right)=\arg\max_{i\in\mathcal{C}}\left(P_i^{\mathrm{rec}}+B_i\right), \tag{11d}$$

$$R_k\left(Z_{\zeta_k}\left(\mathcal{B}\right),\gamma_{k,\zeta_k}\left(B_{\zeta_k}\right)\right)>R_{\mathrm{thresh}},\ k\in\mathcal{U}, \tag{11e}$$

where the objective function (11a) is the network energy efficiency and the optimization variable is the cell-association bias set. Eqs. (11b) and (11c) are the cell-association bias adjustment constraints of the macrocell and picocell, respectively. Eq. (11d) indicates that the users' serving cell is altered by the cell-association bias changes during the optimization. Eq. (11e) is the users' data rate constraint. Because of the dynamic variations of the serving cell and the nature of energy efficiency, the formulated optimization problem cannot be transformed into a convex form and the optimization problem is an NP-hard problem. The proof of the NP-hardness can be summarized as follows. If we relax (11b) and (11c) into a reduced form, the reduced form can be regarded as a user association problem, which can be proved as a K-media problem. Details of the K-media problem and the NP-hardness proof can be found in [28]. Considering the NP-hardness of problem (11), it is difficult to find the optimal solution using conventional algorithms owing to the convergence speed and trap into the local optimal solution. Thus, to solve this problem, we propose two energy-efficient Gibbs sampling based cell-association bias adjustment algorithms.

4 Energy-efficient Gibbs sampling based cell-association bias adjustment algorithm

In this section, we propose a CGSCA that is based on global information to solve the optimization problem (11). Then, considering the overhead of the exchanged information and implementation complexity, we propose a DGSCA. To facilitate the understanding of the CGSCA and DGSCA algorithms, we first introduce the fundamental elements and notions of Gibbs sampling, and we then give details of the CGSCA and DGSCA algorithms.

4.1 Gibbs sampling algorithm

Gibbs first proposed the Gibbs sampling technique in 1902, and he then used it to model and analyze the physical interaction between particles and molecules. Over time, the original Gibbs sampling model has been used to estimate the posterior mode in image processing optimization [29], and to optimize the network throughput in wireless networks [24]. More specifically, Gibbs sampling can be used to solve the optimization problem as follows:

$$e^* = \min_{\boldsymbol{x}\in\mathcal{X}} E\left(\boldsymbol{x}\right), \tag{12}$$

where $\boldsymbol{x}$ is an optimization variable row vector, where each element x_n $(n = 1, 2, \ldots, N)$ is in a discrete set and the feasible domain comes from the Cartesian product. The optimization objective function E can be of any form. The Gibbs sampling algorithm updates the state of each discrete variable x_n iteratively following the Gibbs sampling probability distribution

$$p_n(\boldsymbol{x}_{-n}) = p_n(x_n|\boldsymbol{x}_{-n}) = \frac{\exp(E(x_n, \boldsymbol{x}_{-n})/-T)}{\sum_{x_n^*\in\mathcal{X}_n}\exp(E(x_n^*, \boldsymbol{x}_{-n})/-T)}, \tag{13}$$

where $\boldsymbol{x}_{-n} = (x_1, \ldots, x_{n-1}, x_{n+1}, \ldots, x_N)$ is the variable vector, with the exception of variable x_n. The value of the optimization variable x_n corresponding to a lower $E\left(x_n, \boldsymbol{x}_{-n}\right)$ will be chosen with a higher probability. The temperature parameter T is a key element to ensure good-quality solution. As the iteration time goes to infinity, the temperature parameter Twill approach zero and the algorithm will converge to the global optimal solution [24].

4.2 Energy-efficient centralized Gibbs sampling based cell-association bias adjustment algorithm

In the CGSCA algorithm, a macrocell is regarded as a central processor that takes charge of central processing and determines the cell-association bias of each small cell using the Gibbs sampling algorithm based on global information, which includes the RSRP of all users from all cells, the SINR of each user, each user's serving cell, and the number of users in each cell. Because there is almost no relationship between the optimization variable and the update order [24], for convenience, we take the round robin as the update order. When it is time to update the cell-association bias set, each user should transmit its RSRP and SINR to its serving cell, and then the feedback information is transmitted to the central macrocell. Considering the difference between the objective function of the Gibbs sampling (12) and our optimization problem (11), the Gibbs sampling probability distribution can be rewritten as follows:

$$p_i(\mathcal{B}_{-i}) = p_i(B_i|\mathcal{B}_{-i}) = \frac{\exp(\eta_{EE}(B_i, \mathcal{B}_{-i})/T)}{\sum_{B_i'\in\mathcal{B}}\exp(\eta_{EE}(B_i', \mathcal{B}_{-i}')/T)}, \tag{14}$$

where p_i is the Gibbs sampling probability distribution of cell i. $\mathcal{B}_{-i}$ is a row vector consisting of the cell-association bias of all cells except cell i. η_{EE} is the objective function of the energy efficiency. From (14), we find that under the row vector of bias $\mathcal{B}_{-i}$, the cell-association bias B_i of cell i corresponding to higher energy efficiency $\eta_{EE}\left(B_i, \mathcal{B}_{-i}\right)$ will be chosen with a higher probability under the row vector of bias $\mathcal{B}_{-i}$.

At time epoch t, the temporary cell-association bias of cell i chosen by (14), which is represented by $B_i^{\text{temp}}\left(t\right)$, and the temporary cell-association bias vector of cells $\mathcal{B}^{\text{temp}}\left(t\right)$ can be expressed as

$$\mathcal{B}^{\text{temp}}\left(t\right) = \left(B_i^{\text{temp}}\left(t\right), \mathcal{B}_{-i}\left(t-\right)\right), \tag{15}$$

where $t-$ is the last time epoch of the cell-association bias adjustment, and is mentioned below as the "before time epoch t". In other words, the current temporary cell-association bias vector is relative to the current temporary cell-association bias of cell i and the cell-association bias vector, with the exception

of cell i before time epoch t. The cell-association bias updated decision criterion can be represented as

$$B_i(t) = \begin{cases} B_i^{\text{temp}}, & \text{if } \eta_{EE}(B_i^{\text{temp}}(t), \mathcal{B}_{-i}(t-)) \geqslant \eta_{EE}(\mathcal{B}(t-)) \text{ and } R(B_i^{\text{temp}}) \geqslant R_{\text{threshold}}, \\ B_i(t-), & \text{otherwise}, \end{cases} \tag{16}$$

where $B_i\,(t)$ and $B_i\,(t-)$ are the cell-association bias at time epoch t and before time epoch t. That is, the cell-association bias will be updated only when the energy efficiency calculated by the current temporary cell-association bias is larger than that calculated by the cell-association bias before time epoch t; meanwhile, the users' data rate can be met. Otherwise, the cell-association bias of cell i at time epoch t will not change, and equal the bias value before time epoch t.

Over time, the macrocell selects the cell-association bias iteratively for all the picocells. After that, the macrocell sends the obtained optimal cell-association bias to each picocell. The optimality proof of the CGSCA algorithm is the same as in [24].

4.3 Energy-efficient distributed Gibbs sampling based cell-association bias adjustment algorithm

Considering the details of the proposed CGSCA algorithm above, the key of CGSCA is to calculate the Gibbs probability distribution (14). As an example, consider cell i. If cell i is the cell that needs to be adjusted, the macrocell has to know all of the possible $\eta_{EE}(\mathcal{Z}(B_i^{\text{temp}}, \mathcal{B}_{-i}(t-)), \gamma(B_i^{\text{temp}}, \mathcal{B}_{-i}(t-)))$, and conducts the central processing to make the decision regarding the cell-association bias adjustment. For convenience, we use B_i as an abbreviation for $B_i^{\text{temp}}(t)$. In order to obtain $\mathcal{Z}(B_i, \mathcal{B}_{-i}(t-))$ and $\gamma(B_i, \mathcal{B}_{-i}(t-))$, each small cell should send back the information about the RSRP of all users from all cells, including the SINR of each user, each user's serving cell, and the number of users in each cell. There would be a significant overhead of exchanged messages, in addition to the implementation complexity required to obtain these sets of information, especially in UDNs. Therefore, we propose a distributed cell-association bias adjustment algorithm with a lower message-exchange overhead and implementation complexity, called the energy-efficient DGSCA. In DGSCA, each small cell is able to calculate relevant information and restore the information that arrives from other cells. There is no central processor to determine the order and the time epoch of each small cell to update its cell-association bias, so each small cell makes its decision in a distributed manner in terms of when to update the cell-association bias. The key point of DGSCA is also the calculation of the Gibbs probability distribution (14). In order to reduce the overhead of the messages exchanged and implementation complexity, we derive the distributed updated formulas of $\mathcal{Z}(B_i, \mathcal{B}_{-i}(t-))$ and $\gamma(B_i, \mathcal{B}_{-i}(t-))$, respectively. Details about the DGSCA algorithm can be summarized as follows:

First, we derive the updated formula of the set of the number of users $\mathcal{Z}(B_i, \mathcal{B}_{-i}(t-))$. In order to obtain $\mathcal{Z}(B_i, \mathcal{B}_{-i}(t-))$, the number of users $Z_i(B_i, \mathcal{B}_{-i}(t-))$ in cell i and in other cells (such as cell j $Z_j(B_i, \mathcal{B}_{-i}(t-))$) should be calculated. Suppose that at time epoch t, it is the order of small cell i to adjust its cell-association bias. If $j = i$, $Z_j(B_i, \mathcal{B}_{-i}(t-)) = Z_i(B_i, \mathcal{B}_{-i}(t-))$, the number of users $Z_j(B_i, \mathcal{B}_{-i}(t-))$ for all possible cell-association bias B_i is updated as

$$\begin{aligned} Z_j(B_i, \mathcal{B}_{-i}(t-)) = Z_j(\mathcal{B}(t-)) &+ \frac{1}{2}\left[1 + \frac{B_i - B_i(t-)}{|B_i - B_i(t-)|}\right] \sum_{k \in \mathcal{U}} \delta(\zeta_k(\mathcal{B}(t-)) \neq j)\delta(\zeta_k(\mathcal{B}(t)) = j) \\ &- \frac{1}{2}\left[1 - \frac{B_i - B_i(t-)}{|B_i - B_i(t-)|}\right] \sum_{k \in \mathcal{U}} \delta(\zeta_k(\mathcal{B}(t-)) = j)\delta(\zeta_k(\mathcal{B}(t)) \neq j), \end{aligned} \tag{17}$$

where $Z_j(\mathcal{B}(t-))$ is the number of users in cell j before time epoch t. $\zeta_k(\mathcal{B}(t-))$ is the serving cell of user k before time epoch t and $\zeta_k(\mathcal{B}(t))$ is the serving cell of user k at time epoch t. $\delta(\cdot)$ is a delta function. If $(\cdot)$ is true, $\delta(\cdot) = 1$; otherwise, $\delta(\cdot) = 0$. $\delta(\zeta_k(\mathcal{B}(t-)) \neq j)\delta(\zeta_k(\mathcal{B}(t)) = j)$ is a user association indicator. If the value of the user-association indicator equals 1, it means that the user k has changed its serving cell from another cell to cell j when cell i chooses B_i at time epoch t; otherwise, the value is 0. From formula (17), we can see that in the case of $j = i$, $Z_j(B_i, \mathcal{B}_{-i}(t-))$ consists of three parts. The first part

is the number of users $Z_j(\mathcal{B}(t-))$ in cell j before cell i adjusts its cell-association bias. The second part is the number of users being transferred from cell j to other cells under the cell-association bias adjustment of cell i. The last part is the number of users being offloaded from other cells to cell j as cell i adjusts its cell-association bias. The users' serving cell is updated as follows:

$$\begin{aligned}\zeta_k(\mathcal{B}(t)) &= \zeta_k(B_i, \mathcal{B}_{-i}(t-)) \\ &= \begin{cases} i, & \text{if } P^{\text{rec}}_{i,k} + B_i > P^{\text{rec}}_{\zeta_k(\mathcal{B}(t-)),k} + B_{\zeta_k(\mathcal{B}(t-))}, \\ \zeta_k(\mathcal{B}(t-)), & \text{if } P^{\text{rec}}_{i,k} + B_i \leqslant P^{\text{rec}}_{\zeta_k(\mathcal{B}(t-)),k} + B_{\zeta_k(\beta(t-))} \text{ and } i \neq \zeta_k(\mathcal{B}(t-)), \\ \arg\max\limits_{c\in C} P^{\text{rec}}_{c,k} + B_c, & \text{if } P^{\text{rec}}_{i,k} + B_i \leqslant P^{\text{rec}}_{\zeta_k(\mathcal{B}(t-)),k} + B_{\zeta_k(\mathcal{B}(t-))} \text{ and } i = \zeta_k(\mathcal{B}(t-)), \end{cases} \end{aligned} \tag{18}$$

where $\zeta_k(\mathcal{B}(t))$ is the updated serving cell of user k under the current temporary cell-association bias of cell i and the cell-association bias set, with the exception of cell i before time epoch t. The updated serving cell can be divided into three cases. First, the serving cell of user k will change into cell i if the BRSRP (according to the cell-association bias B_i) from cell i is larger than that from the original serving cell before time epoch t. Secondly, the serving cell of user k will not change with the cell-association bias adjustment of cell i if the BRSRP is less than that received from the original serving cell before time epoch t and the cell i is not the original serving cell of user k. Finally, the serving cell will change to the cell that can provide the maximum received signal power if the BRSRP from cell i is not larger than that from the original serving cell before time epoch t, and if cell i is the original serving cell of user k.

Similar to the case of $j = i$, if $j \neq i$, the number of users $Z_j(B_i, \mathcal{B}_{-i}(t-))$ for all possible cell-association bias B_i can be updated as

$$\begin{aligned} Z_j(B_i, \mathcal{B}_{-i}(t-)) = Z_j(\mathcal{B}(t-)) &- \frac{1}{2}\left[1 + \frac{B_i - B_i(t-)}{|B_i - B_i(t-)|}\right] \sum_{k\in\mathcal{U}} \delta(\zeta_k(\mathcal{B}(t-)) = j)\delta(\zeta_k(\mathcal{B}(t)) = i) \\ &+ \frac{1}{2}\left[1 - \frac{B_i - B_i(t-)}{|B_i - B_i(t-)|}\right] \sum_{k\in\mathcal{U}} \delta(\zeta_k(\mathcal{B}(t-)) = i)\delta(\zeta_k(\mathcal{B}(t)) = j). \end{aligned} \tag{19}$$

From the formula (19), we can see that $Z_j\left(B_i, \mathcal{B}_{-i}\left(t-\right)\right)$ consists of three parts. The first one is the original number of users $Z_j\left(\mathcal{B}\left(t-\right)\right)$ before the cell-association bias adjustment. The second one is the number of users whose serving cells are changed from cell j to cell i. The last one is the number of users being transferred from cell i to cell j.

From the above discussion, we can see that in order to calculate the set of the number of users $\mathcal{Z}\left(B_i, \mathcal{B}_{-i}\left(t-\right)\right)$ served by the cells, each cell can utilize formula (17)–(19) to calculate the change in the number of users and to estimate the alteration of the users' serving cells. Specifically, each cell should follow the order to update its cell-association bias, and should consider whether it is the appropriate time for updating the cell-association bias. At time epoch t, if cell j is to update its cell-association bias, cell j should first estimate the potential serving cell alteration of its users according to the recorded BRSRP before time epoch t. Then, other cells should predict the possible changes of their users' serving cells when cell j adjusts its cell-association bias. If some users' serving cells vary, a new serving cell should be communicated to the users. If it is not the order of cell j, cell j only needs to predict the serving cell changes of its serving users. Finally, each cell will know the number of users served by itself when cell j adjusts its cell-association bias, and hence we obtain $\mathcal{Z}\left(B_j, \mathcal{B}_{-j}\left(t-\right)\right)$.

Secondly, the calculation of the variation in the SINR $\gamma\left(B_i, \mathcal{B}_{-i}\left(t-\right)\right)$with the cell-association bias adjustment can be summarized as follows. At time epoch t, there are two cases regarding the serving cell of user k if it is the order of cell i to adjust its cell-association bias. In the first case, if cell i is just the serving cell of user k, the SINR of user $k$can be updated as follows:

$$\begin{aligned} \gamma_k(B_i, \mathcal{B}_{-i}(t-)) = \frac{1}{2}&\left[1 + \frac{B_i - B_i(t-)}{|B_i - B_i(t-)|}\right] \gamma_k(\mathcal{B}(t-)) + \frac{1}{2}\left[1 - \frac{B_i - B_i(t-)}{|B_i - B_i(t-)|}\right] \delta(\zeta_k(B_i) = i)\gamma_k(\mathcal{B}(t-)) \\ &+ \frac{1}{2}\left[1 - \frac{B_i - B_i(t-)}{|B_i - B_i(t-)|}\right] \delta(\zeta_k(B_i) \neq i) \times \frac{P^{\text{rec}}_{\zeta_k(B_i),k}}{P^{\text{rec}}_{i,k}/\gamma_k(\mathcal{B}(t-)) - P^{\text{rec}}_{\zeta_k(B_i),k} + P^{\text{rec}}_{i,k}}, \end{aligned} \tag{20}$$

where $\gamma_k(\mathcal{B}(t-))$ is the SINR of user k under the cell-association bias set $\mathcal{B}$ before time epoch t. $P_{i,k}^{\text{rec}}$ and $P_{\zeta_k(B_i),k}^{\text{rec}}$ are the RSRP of user k from cell i and cell $\zeta_k(B_i)$, respectively. We know that γ_k is only relative to the user's serving cell changed if the transmission power of the serving cell is unchanged. Therefore, there are two conditions that affect γ_k. The first condition is that the serving cell is unchanged as the cell-association bias adjustment. In this case, as the cell-association bias increases ($B_i > B_i(t-)$), the serving cell of user k will be unchanged and γ_k will be the same as that in the last moment, as in the first part of formula (20). Then, although the cell-association bias decreases, the serving cell of user k is unchanged. The SINR will not be changed, as in the second part of formula (20). The second condition is that the serving cell changes with the cell-association bias adjustment. In this case, similar to the third part of formula (20), as the cell-association bias decreases ($B_i < B_i(t-)$), the serving cell changes from cell i to cell $\zeta_k(B_i)$, which causes γ_k to be changed. Details of the derivation of the third part of formula (20) can be expressed as follows:

$$\begin{aligned}\gamma_k(B_i,\mathcal{B}_{-i}(t-)) &= \frac{P_{\zeta_k(B_i)}G_{\zeta_k(B_i),k}}{\sum_{j\in\mathcal{C}/\zeta_k(B_i)}P_jG_{j,k}+N_0} = \frac{P_{\zeta_k(B_i)}G_{\zeta_k(B_i),k}}{\frac{P_iG_{i,k}}{P_iG_{i,k}/\sum_{j\in\mathcal{C}/i}P_jG_{j,k}+N_0}-P_{\zeta_k(B_i)}G_{\zeta_k(B_i),k}+P_iG_{i,k}}\\ &= \frac{P_{\zeta_k(B_i)}G_{\zeta_k(B_i),k}}{P_iG_{i,k}/\gamma_k(\mathcal{B}(t-))-P_{\zeta_k(B_i)}G_{\zeta_k(B_i),k}+P_iG_{i,k}}.\end{aligned} \tag{21}$$

In the second case, if it is the order of cell i to update the cell-association bias, the SINR of user k served by cell j can be expressed as

$$\begin{aligned}\gamma_k(B_i,\mathcal{B}_{-i}(t-)) &= \frac{1}{2}\left[1-\frac{B_i-B_i(t-)}{|B_i-B_i(t-)|}\right]\gamma_k(\mathcal{B}(t-))+\frac{1}{2}\left[1+\frac{B_i-B_i(t-)}{|B_i-B_i(t-)|}\right]\delta(\zeta_k(B_i)=j)\gamma_k(\mathcal{B}(t-))\\ &\quad+\frac{1}{2}\left[1+\frac{B_i-B_i(t-)}{|B_i-B_i(t-)|}\right]\delta(\zeta_k(B_i)=i)\times\frac{P_{i,k}^{\text{rec}}}{P_{j,k}^{\text{rec}}/\gamma_k(\mathcal{B}(t-))-P_{i,k}^{\text{rec}}+P_{j,k}^{\text{rec}}}.\end{aligned} \tag{22}$$

From the above formula derivation, we can see that γ_k can be obtained from Formula (20) and (22). From the derivation, any cell should identify whether it is the updating cell or the common cell. If cell j is just the updating cell, cell j needs only to record the RSRP of the serving users, the users' potential serving cells, and the users' SINR before time epoch t. Otherwise, if cell j is not the updating cell, cell j needs only to record the users' RSRP from cell i and cell j, as well as the SINR of its users before time epoch t.

Up to the present, we have obtained the number of users $\mathcal{Z}(B_i,\mathcal{B}_{-i}(t-))$ and the SINR $\gamma(B_i,\mathcal{B}_{-i}(t-))$ when cell i wants to adjust its cell-association bias B_i at time epoch t. Further, from the Formula (10), we can obtain the energy efficiency. After that, we can calculate the updated cell-association bias of cell i according to the Formula (14) and (16). From the derivation of the formula, the DGSCA algorithm does not need to know the global information. The waiting cell-association bias adjustment cell only needs a small amount of updated information from other cells, such as the updated number of users, changes to the users' serving cell, and the updated SINR. In addition, the optimality of CGSCA and DGSCA can be shown to be similar to the method provided in literature [24], so we do not give the detailed proof here. Considering that the user cannot perform frequent handovers, only if there are changes that are caused by the users' distribution or the small cell redeployment, and if the handover interval is met [26] will the cell-association bias of CGSCA and DGSCA be adjusted. Because it is difficult to evaluate precisely the signaling latency caused by non-ideal backhaul, the effects of signaling latency are usually not mentioned in studies on the cell-association bias adjustment, as in [17, 19, 21, 27]. Therefore, the effects of signaling latency caused by non-ideal backhaulare not considered in this paper.

5 Complexity analysis

In this section, we analyze the computational complexity of the proposed CGSCA, DGSCA, and the tier-specific cell-association bias adjustment scheme. The required computational complexity (the number of

Table 1 Computational complexity analysis

Parameters	Computational complexity		
	CGSCA	DGSCA	Tier-specific
RSRP	$N_M + N_P$	$\begin{cases} N_M + N_P, & \text{if } j = i \\ 2, & \text{if } j \neq i \end{cases}$	$N_M + N_P$
Serving cell	$N_M + N_P$	$\begin{cases} N_M + N_P, & \text{if } j = i \\ 2, & \text{if } j \neq i \end{cases}$	$N_M + N_P$
Achievable rates of all users	$N_U\,(2N_M + 2N_U + 3)$	$\leqslant \sum\limits_{j \neq i} 9U_j + U_i\,(2N_M + 2N_P + 4)$	$N_U\,(2N_M + 2N_U + 3)$
The decision of cell-association bias of each iteration	$N_b N_U\,(N_M + N_P + 3) + N_b + N_M + N_P$	$\leqslant N_b\left(\sum_{j \neq i} 9U_j + 1\right) + N_b U_i\,(N_M + N_P + 4) + N_M + N_P$	$N_U\,(2N_M + 2N_U + 3)$

multiplications and divisions performed during the processing of the algorithms) of different algorithms is compared in Table 1 when cell i adjusts its cell-association bias.

Set the total number of cell-association bias as N_b, which can be calculated by $N_b = (B_{\max} - B_{\min})/\Delta + 1$ and Δ is the adjustment step. In the case of UDNs, $N_M + N_P > 6$ and $\sum_{j \neq i} U_j > U_i$. Therefore, we can obtain the following inequation

$$\begin{aligned} N_U\,(N_M + N_P + 3) &= \sum_{j \neq i} U_j\,(N_M + N_P + 3) + U_i\,(N_M + N_P + 3) \\ &= \sum_{j \neq i} 9U_j + U_i\,(N_M + N_P + 4) + \sum_{j \neq i} U_j\,(N_M + N_P - 6) - U_i \\ &> \sum_{j \neq i} 9U_j + U_i\,(N_M + N_P + 4)\,. \end{aligned} \tag{23}$$

From Formula (23), we determine that the computation complexity of the DGSCA is lower than CGSCA in each iteration. This means that as the network scale expands, the DGSCA can result in reduced computation complexity compared with CGSCA. From Table 1, we see that the decisions of the cell-association bias configuration of the proposed CGSCA and DGSCA algorithms result in a linear increase in the computational complexity as the scale of the network increases and hence it is feasible for them to be utilized in large scale deployment scenarios, such as UDNs.

In addition, we analyzed the communication complexity of the proposed CGSCA and DGSCA algorithms in terms of the signal-exchange overhead from the perspective of the RSRP, cell-association bias configuration, and energy efficiency update information. The signal-exchange overhead often occurs between users and their serving cells. From the complexity analysis above, the required communication complexities of these two algorithms are $\mathcal{O}(N_U(N_M + N_P) + 1)$ and $\mathcal{O}(2\sum_{j \neq i} U_j + (U_i + 1)(N_M + N_P) + 1)$, respectively.

6 Simulation results and performance analysis

In this section, we present numerical results to validate the proposed CGSCA and DGSCA algorithms by making comparisons with existing cell-association bias adjustment algorithms. The first one is the commonly used trial-and-error method, where all of the picocells adopt an identical cell-association bias in the optimization, and is labeled as equal search cell-association bias adjustment (ESCA). The second one, which is denoted as the respective search cell-association bias adjustment (RSCA), is that each picocell chooses its cell-association bias value using the Q-learning algorithm. The respective search best selection cell-association bias adjustment (RSBSCA) is the third one, and is applied to test the convergence performance of RSCA. The fourth one is the no cell-association bias adjustment (NCA),

Table 2 Simulation parameters

Parameter	Value
Transmission power of macrocell and picocell (mW)	20000 and 130
Bandwidth W (MHz)	10
Carrier frequency (GHz)	2
Maximum and minimum cell-association bias (dB)	16 and -16
Power consumption of macrocell in ideal mode (mW)	1300000
Power consumption of picocell in ideal and sleep mode (mW)	6800 and 4300
Reciprocal of power amplifier efficiency of macrocell and picocell	4.7 and 4
Antenna gain	Macrocell: 3D antenna gain Picocell: 5 dBi
Shadow standard deviation	Macrocell: 8 dB; picocell: 10 dB
Path loss R (km)	Macrocell: 128.1+37.6log10(R) dB Picocell: 140.7+36.7log10(R) dB

where each picocell does not adjust the cell-association bias configuration. The fifth one is the exhaustive search cell-association bias adjustment (EXSCA), where the cell-association bias adjustment scale is set as 1dB in the search step using the exhaustive search algorithm. To verify the robustness of the proposed algorithms, and to show the effects of a possible transmission error, the performances of CGSCA and DGSCA under the scenario of a 5% transmission error are considered in the simulations, and are labeled as CGSCATE and DGSCATE, respectively. The simulation parameters, which are shown in Table 2, are in accordance with the EARTH project [11] and the 3GPP Technical Specification [22]. The simulation scenario is described as follows: there are some picocell clusters deployed in one sector of the center macrocell in a 19-site network. Two thirds of users are randomly distributed in the coverage of the clustered picocell, and the remaining one third of users is randomly distributed in the macrocell sector. The threshold of the users' data rate R_{thresh} is chosen by setting the bias of all the picocells as $B_i = 0,\ i \in \mathcal{C}$. We only used the threshold to test whether our proposed algorithms are sensitive to the users' data rate constraint, and the threshold can be set to other values for further discussion. In the simulation, we obtain the results by averaging several independent simulations.

6.1 Convergence performance of energy efficiency

In this subsection, to verify the effectiveness of the proposed algorithms and analyze the importance of users' data rate constraint in the energy efficiency optimization, we investigate the convergence performance of the energy efficiency with and without the users' data rate constraint. To test whether the proposed CGSCA and DGSCA algorithms can converge to the optimal solution, we denote the final results of the EXSCA as the optimal solution and refer to it as the optimal solution of cell-association bias adjustment (OSCA). The convergence performances of the energy efficiency without the users' data rate constraint are shown in Figure 1. Considering the computation complexity and the time complexity of the EXSCA exponential increase with the scale of picocells, as an example, we employ five picocells and 120 users in one sector of a macrocell, and 100 iterations of all algorithms. During the simulation process, we obtained the simulation results of the first iteration time by setting the cell-association bias as 0 dB or the minimum value in different algorithms. Once an optimization algorithm works, the network energy efficiency will be improved significantly. Therefore, there exists a burst-like increase in the following iterations. In addition, because of the mechanism of Gibbs sampling, the proposed CGSCA and DGSCA algorithms can converge to the optimal solution more rapidly than other algorithms. The ESCA algorithm also has a fast convergence speed, but there is a performance gap between its convergence results and the optimal solution. Although there exists a growing trend of the RSCA algorithm, it has a slower convergence speed compared to the proposed two algorithms. The EXSCA algorithm has the slowest convergence speed although it can also converge to the optimal solution. This is because each potential cell-association bias solution has to be tried for all of the picocells. Although in CGSCATE

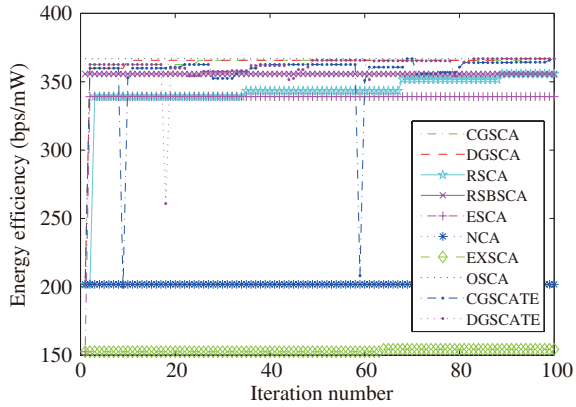

Figure 1 (Color online) Energy efficiency without data rate constraint.

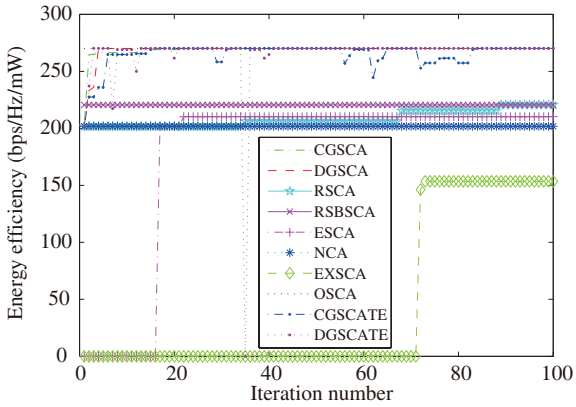

Figure 2 (Color online) Energy efficiency with data rate constraint.

and DGSCATE, there are some decreased values caused by transmission errors, the performance of the proposed algorithms can converge to the best value after a few iterations.

In Figure 2, we compare the convergence performances of the energy efficiency for different solutions with the users' data rate constraint. From the figure, we can see that the proposed CGSCA and DGSCA algorithms have a faster convergence speed and can converge to the optimal solution. Meanwhile, the RSCA algorithm has a slower convergence speed. The result of the ESCA algorithm is zero at the beginning, and then it increases as the number of iterations increases, and finally converges. This is because the ESCA algorithm applies an identical cell-association bias to all picocells during the optimization process. The users' data rate requirement cannot be met if the chosen cell-association bias value is low, and hence the energy efficiency is zero.

Combining Figure 1 and Figure 2, we find that the CGSCA and DGSCA algorithms have a faster convergence speed, and is guaranteed to converge to the optimal solution regardless of the users' data rate constraint. However, there is a performance gap between the energy efficiency with and without the data rate constraint. The optimal solution with the data rate constraint is lower than that without the data rate constraint. This is because if there is no constraint in the users' data rate, the resource allocation for the whole network tends to maximize the energy efficiency by keeping the throughput performance gain larger than the energy consumption, and turning off as many picocells as possible. If there is user's data rate constraint, the resource allocation should first meet the constraint of all of the users' data rates, and then maximize the energy efficiency. That is, if the users' data rate constraint is not considered in the energy-efficiency optimization, some users' performance will be sacrificed to maximize the energy efficiency. Therefore, the users' data rate constraint is essential to energy efficiency optimization.

6.2 Throughput convergence performance

In this subsection, we investigate the convergence performance of the throughput with and without the users' data rate constraint. From Figure 3, we find that the proposed CGSCA and DGSCA algorithm can converge to the optimal solution and can have a better optimal solution compared with other algorithms owing to the Gibbs sampling mechanism. The ESCA algorithm has a faster convergence speed, but there is a performance gap between the converged value and the optimal solution.

The convergence performances of the throughput with the users' date rate constraint are shown in Figure 4. The proposed CGSCA and DGSCA algorithms can converge to the optimal solution quickly, and have higher gain compared with the ESCA and RSCA algorithms. For a small number of iterations, the throughput of the ESCA algorithm is zero, and it then increases, finally converging to its best solution. This is because, at the beginning, the ESCA algorithm adopts the equal the identical cell-association bias of picocells in the optimization, which prevents the users' data rate requirement from being met, and the throughput is zero.

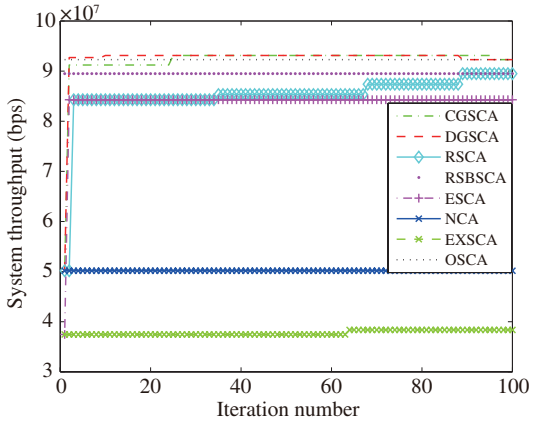

Figure 3 (Color online) Throughput without data rate constraint.

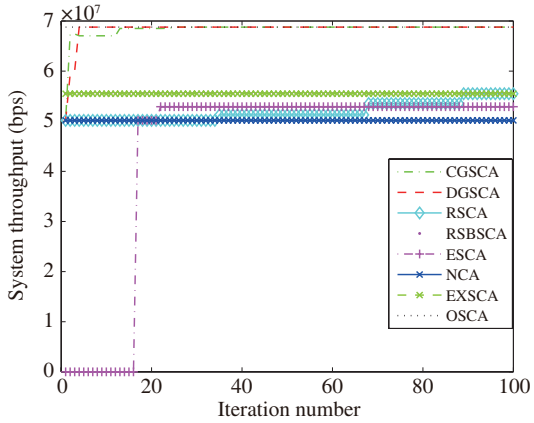

Figure 4 (Color online) Throughput with data rate constraint.

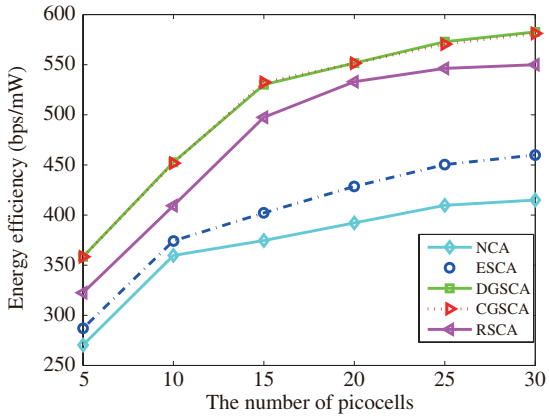

Figure 5 (Color online) Variation in energy efficiency with an increasing number of picocells.

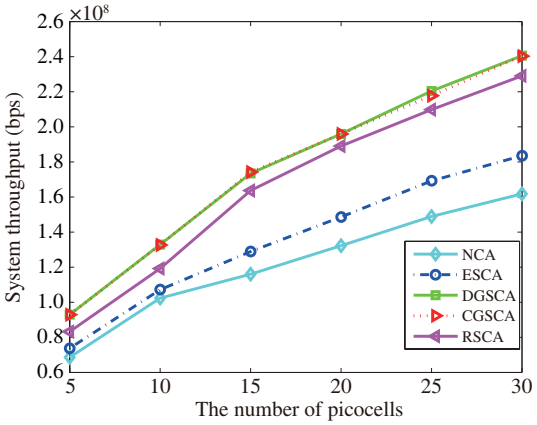

Figure 6 (Color online) Variation of throughput with an increasing number of picocells.

6.3 Variation in energy efficiency and throughput performances with an increasing number of picocells

In the previous subsection, we analyzed the convergence performance of the energy efficiency and throughput with and without date rate constraint. We determined that there is a performance gap between the performances with and without data rate constraint, and it is necessary to further study the energy efficiency and throughput with the users' data rate constraint as the number of picocells increases. From the simulation results in Figure 5, we see that the energy efficiency increases as the number of picocells increases. However, as the number of picocells further increases, there is a slowing of the growth trend. This is because the ICI and the energy consumption of the network increase with an increasing number of picocells. The RSCA algorithm has better results compared with the ESCA and NCA algorithms, but the convergence is much slower than the proposed CGSCA and DGSCA algorithms according to Figure 2.

In Figure 6, we investigate the throughput performance as the number of picocells increases. From the figure, we can see that the growing trend of the performance gain slows with the increasing number of picocells because of the increasing ICI. Although the other algorithms have a similar performance trend, CGSCA and DGSCA algorithms exhibit the best performance gain. In addition, considering that the theory of CGSCA and DGSCA algorithms are based on the Gibbs sampling, CGSCA and DGSCA algorithms therefore have the same performance in Figures 5 and 6.

6.4 Cumulative distribution function of performance

In this subsection, we compare the throughput CDF performance for different numbers of picocells under DGSCA and NCA algorithms. In order to distinguish between these results, we employ the log-scale for

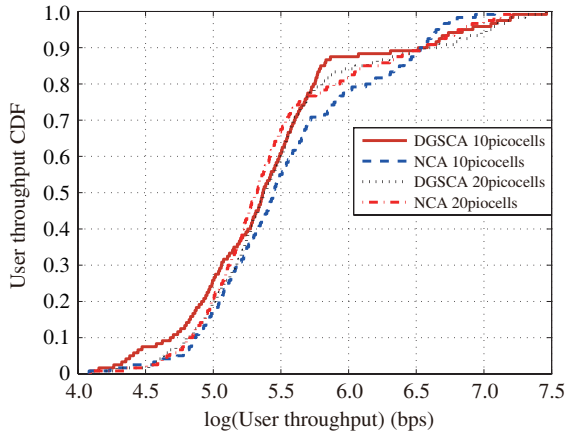

Figure 7 (Color online) User throughput CDF.

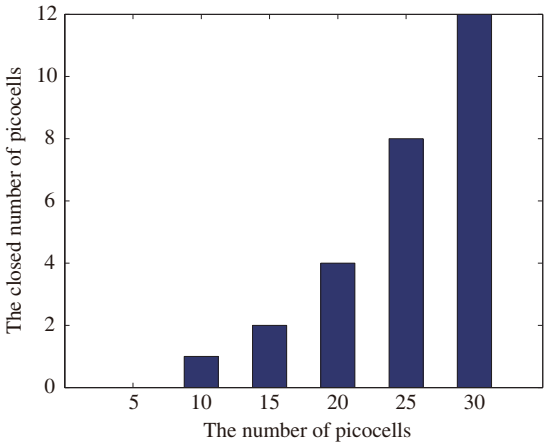

Figure 8 (Color online) Number of shutdown picocells for DGSCA algorithm.

the x-axis in Figure 7. From this figure, we can see that for the same number of picocells, the throughput performance of most users is improved and the performance curves intersect at about 6.5, which means that the data rates of a few users decreased. This is because by adjusting the cell-association bias, some users are offloaded from low-load picocells to other picocells or macrocells to enable the shutting down of the original picocells, leading to energy savings. Further, the offloaded users may expropriate the available resource blocks of some users, which results in a deterioration in the data rate of some users to realize improved energy efficiency.

6.5 Number of shutdown picocells for DGSCA algorithm

In this subsection, we consider the performance of the number of shutdown picocells for the DGSCA algorithm as the number of picocells increases. From Figure 8, we can see that there is an increase in the number of closed picocells as the number of picocells increased. This is because for the same number of users, there is an increase in the ICI and network energy consumption as the number of picocells increases. In other words, an increasing number of picocells is not always advantageous from energy efficiency perspective.

7 Conclusion

In this paper, we proposed an energy-efficient cell-association bias adjustment scheme to maximize the energy efficiency for UDNs while considering the influence of the users' data rate constraint in the optimization. First, we formulated an energy efficiency maximization problem by adjusting the cell-association bias, while considering the users' data rate constraint. Then, we proposed a CGSCA algorithm with global information. To reduce the overhead of the exchanged messages and the computation complexity caused by the increasing network scale, we further proposed a DGSCA algorithm. In DGSCA, the decision is made by each picocell, and only some of the updated information is exchanged between picocells. Finally, the simulation results show that the two proposed energy-efficient Gibbs sampling based cell-association bias adjustment algorithms have a faster convergence speed and a better performance gain in terms of the energy efficiency and system throughput, compared to existing algorithms with and without users' data rate constraint.

Acknowledgements This research was supported by National Natural Science Foundation of China (Grant No. 61471114), Research Fund of the National Mobile Communications Research Laboratory, Southeast University (Grant No. 2017A03), and Nature Research Fund for Key Project of Anhui Higher Education (Grant No. KJ2016A455).

Conflict of interest The authors declare that they have no conflict of interest.

References

1 You X H, Pan Z W, Gao X Q, et al. The 5G mobile communication: the development trends and its emerging key techniques (in Chinese). Sci Sin Inform, 2014, 44: 551–563
2 Venturino L, Zappone A, Risi C, et al. E nergy-efficient scheduling and power allocation in downlink OFDMA networks with base station coordination. IEEE Trans Wirel Commun, 2015, 14: 1–14
3 Osseiran A, Boccardi F, Braun V, et al. Scenarios for 5G mobile and wireless communications: the vision of the METIS project. IEEE Commun Mag, 2014, 52: 26–35
4 Yang C G, Li J D, Guizani M. Cooperation for spectral and energy efficiency in ultra-dense small cell networks. IEEE Wirel Commun, 2016, 23: 64–71
5 Cai S J, Che Y L, Duan L J, et al. Green 5G heterogeneous networks through dynamic small-cell operation. IEEE J Sel Areas Commun, 2016, 34: 1103–1115
6 Ng D, Lo E, Schober R. Energy-efficient resource allocation in OFDMA systems with hybrid energy harvesting base station. IEEE Trans Wirel Commun, 2013, 12: 3412–3427
7 Han C Z, Harrold T, Armour S, et al. Green radio: radio techniques to enable energy-efficient wireless networks. IEEE Commun Mag, 2011, 49: 46–54
8 Ge X H, Tu S, Mao G Q, et al. 5G ultra-dense cellular networks. IEEE Wirel Commun, 2016, 23: 72–79
9 Ge X H, Ye J L, Yang Y, et al. User mobility evaluation for 5G small cell networks based on individual mobility model. IEEE J Sel Areas Commun, 2016, 34: 528–541
10 Miao G W, Himayat N, Li G Y. Energy-efficient link adaptation in frequency-selective channels. IEEE Trans Commun, 2010, 52: 545–554
11 Auer G, Blume O, Giannini V, et al. Energy efficiency analysis of the reference systems, areas of improvements and target breakdown. Technical Report. EARTH Project. D2.3 V2
12 Cui Q M, Cui Z Y, Zheng W, et al. Energy-aware deployment of dense heterogeneous cellular networks with QoS constraints. Sci China Inf Sci, 2017, 60: 042303
13 Jin Y H, Qiu L, Liang X W. Small cells on/off control and load balancing for green dense heterogeneous networks. In: Proceedings of IEEE Wireless Communications and Networking Conference (WCNC), New Orleans, 2015. 1530–1535
14 Zhao X S, Wang C. An asymmetric cell selection scheme for inter-cell interference coordination in heterogeneous networks. In: Proceedings of IEEE Wireless Communications and Networking Conference (WCNC), Shanghai, 2013. 1226–1230
15 Sun X, Wang S W. Resource allocation scheme for energy saving in heterogeneous networks. IEEE Trans Wirel Commun, 2015, 14: 4407–4416
16 Hossain E, Rasti M, Tabassum H, et al. Evolution toward 5G multi-tier cellular wireless networks: an interference management perspective. IEEE Wirel Commun, 2014, 21: 118–127
17 Okino K, Nakayama T, Yamazaki C, et al. Pico cell range expansion with interference mitigation toward LTE-advanced heterogeneous networks. In: Proceedings of IEEE International Conference on Communications Workshops (ICC), Kyoto, 2011. 1–5
18 Bhushan N, Li J Y, Malladi D, et al. Network densification: the dominant theme for wireless evolution into 5G. IEEE Commun Mag, 2014, 52: 82–89
19 Jo H-S, Sang Y J, Xia P, et al. Heterogeneous cellular networks with flexible cell association: a comprehensive downlink SINR analysis. IEEE Trans Wirel Commun, 2012, 11: 3484–3495
20 Wu Y P, Cui Y, Clerckx B. Analysis and optimization of inter-tier interference coordination in downlink multi-antenna HetNets with offloading. IEEE Trans Wirel Commun, 2015, 14: 6550–6564
21 Qin M L, Liu N, Jiang H L, et al. MPSO-based power adjustment and user association algorithm for energy efficiency in LTE heterogeneous networks. In: Proceedings of 6th International Conference on Wireless Communications and Signal Processing (WCSP), Hefei, 2014. 1–6
22 3GPP. 3rd Generation Partnership Project. Technical specification group radio access network; Further advancements for E-UTRA physical layer aspects (Release 9). Technical Specification 36.814 V9.0.0. 2010
23 Abuzainab N, Vinnakota S, Touati C. Coalition formation game for cooperative cognitive radio using Gibbs sampling. In: Proceedings of IEEE Wireless Communications and Networking Conference (WCNC), New Orleans, 2015. 937–942
24 Qian L P, Zhang Y J, Chiang M. Distributed nonconvex power control using Gibbs sampling. IEEE Trans Commun, 2012, 60: 3886–3898
25 Garcia V, Chen C S, Zhou Y Q, et al. Gibbs sampling based distributed OFDMA resource allocation. Sci China Inf Sci, 2014, 57: 042302
26 Liu F, Mahonen P, Petrova M. A handover scheme towards down-link traffic load balance in heterogeneous cellular networks. In: Proceedings of IEEE International Conference on Communications (ICC), Sydney, 2014. 4875–4880
27 Ye Q Y, Rong B Y, Chen Y D, et al. User association for load balancing in heterogeneous cellular networks. IEEE Trans Wirel Commun, 2013, 12: 2706–2716
28 Jiang H L, Pan Z W, Liu N, et al. LD-IMPSO Based power adjustment algorithm for eICIC in QoS constrained hyper dense HetNets. Wirel Personal Commun, 2016, 88: 111–131
29 Geman S, Geman D. Stochastic relaxation, Gibbs distributions, and the Bayesian restoration of images. IEEE Trans Pattern Anal Mach Intell, 1984, 6: 721–741